Journal of Molecular Spectroscopy **212,** 22–31 (2002)
doi:10.1006/jmsp.2001.8519, available online at http://www.idealibrary.com on IDEAL®

High-Temperature Infrared Emission Spectra of $D^{12}C^{14}N$ and $D^{13}C^{14}N$

E. Möllmann,*,[1] A. G. Maki,† M. Winnewisser,*,[2] B. P. Winnewisser,*,[2] and W. Quapp‡

*Physikalisch-Chemisches Institut, Justus-Liebig-Universität Gießen, Heinrich-Buff-Ring 58, D-35392 Gießen, Germany; †15012 24 Avenue S.E., Mill Creek, Washington 98012-5718; and ‡Mathematisches Institut, Universität Leipzig, Augustus-Platz 10-11, D-04109 Leipzig, Germany

Received July 20, 2001; in revised form December 20, 2001

The infrared spectra of two isotopomers of deuterium cyanide, $D^{12}C^{14}N$ and $D^{13}C^{14}N$, were measured in emission at temperatures of 1370 K and 1520 K, respectively, in the range from 450 to 850 cm^{-1} and, for $D^{12}C^{14}N$, also from 1800 to 2800 cm^{-1}. Assignments were made for rovibrational transitions to high bending states, $v_2 = 9$ for $D^{13}C^{14}N$ and $v_2 = 11$ for $D^{12}C^{14}N$. To aid and verify the assignments, bands of the lower bending states, up to $v_2 = 3$, were also measured in absorption at room temperature. A global fit was made of all measurements available to us for each isotopomer. In addition to giving the rovibrational constants for each state measured, the power series expansion constants are also given and compared with those of the other deuterium cyanide isotopomers. The $D^{12}C^{14}N$ laser transitions are verified as arising from the consequences of the Coriolis interaction between the $J = 21$ levels of the 02^02 and $09^{1e}0$ states.

Key Words: DCN, IR spectroscopy; emission measurements; high-temperature measurements; deuterium cyanide; molecular spectroscopy; DCN laser.

INTRODUCTION

It is widely believed that the reaction path of the isomerization between hydrogen cyanide and hydrogen isocyanide takes place along the bending coordinate of hydrogen cyanide (*1*). This and the simplicity of hydrogen cyanide have given rise to many studies of the potential barrier for this isomerization (*2–4*) and of the bending motions of hydrogen cyanide (*5–7*) and hydrogen isocyanide (*8–10*), of which only a few are mentioned in the references.

Though the spectrum of hydrogen cyanide and the underlying potential function of the isomerization was of great interest, a potential function reaching from the hydrogen cyanide to the hydrogen isocyanide has not yet been published with spectroscopic accuracy (*11*). In an attempt to guide the closing of this gap in the theory, measurements of highly excited hydrogen cyanide and its various isotopomers have been made in the Giessen Laboratory. The current measurements deal with the spectrum of $D^{12}C^{14}N$ and $D^{13}C^{14}N$ in the range of the bands of the bending motion from 450 to 850 cm^{-1} and those of the stretching motions of $D^{12}C^{14}N$ in the range from 1800 to 2800 cm^{-1}. The transitions in the higher wavenumber range were found as an accidental impurity in an emission spectrum of HCN used for HNC measurements (*12*). The $D^{12}C^{14}N$ spectra were thermally excited to temperatures of 1370 K while the $D^{13}C^{14}N$ spectrum was at a temperature of 1520 K. A new oven was used for the higher temperature measurements along with a new ceramic emission cell. The oven was capable of heating the cell to 2000 K. It was equipped with a controlling device that allowed the heating to be adjusted by an external PC (personal computer) according to a previously set heating program.

Until these measurements, there seem to have been only five works reporting the rotationally resolved spectrum of $D^{13}C^{14}N$ (*13–17*). The earlier rovibrational transitions of $D^{13}C^{14}N$ were measured as impurity lines in absorption measurements that were dominated by other isotopomers (*16, 17*). In an earlier report of the absorption measurements used here (*18*) the analysis could be carried on up to the third bending vibrational level of $D^{13}C^{14}N$.

A number of earlier measurements have been reported on the infrared and millimeter wave spectrum of $D^{12}C^{14}N$. The most recent also involved a summary of the results for all data on the isotopomers of DCN available at that time (*18*).

Six laser transitions have been observed for $D^{12}C^{14}N$. Those transitions (*19*) were attributed to the relatively high vibrational states 02^02 and 09^10 which can now be quite accurately described. The present work verifies the assignment of the laser transitions and makes use of the very accurate frequency measurements for five of those transitions to better describe the 02^02 and $09^{1e}0$ levels.

In addition to the emission measurements in this work, absorption measurements were made in the bending fundamental region in order to calibrate the emission spectra and provide better measurements on the lowest bending levels.

Supplementary data for this article are available on IDEAL (http://www.idealibrary.com) and as part of the Ohio State University Molecular Spectroscopy Archives (http://msa.lib.ohio-state.edu/jmsa_hp.htm).

[1] Present address: Gerlachstrasse 18, D-52064 Aachen, Germany.

[2] Present address: Department of Physics, Ohio State University, Columbus, Ohio 43210.

0022-2852/02 $35.00

EXPERIMENTAL DETAILS

The spectra were measured with the Fourier transform spectrometer Bruker IFS 120 HR. It was equipped with a liquid-helium-cooled Ge : Cu detector and a 3.5-μm Mylar beam splitter. The whole optical system was evacuated during the measurements.

For the absorption measurements a multipass absorption cell made of borosilicate glass and sealed with KBr windows was used. A total absorption pathlength of 338 cm was realized with four passes through the cell. The parameters for the measurements are listed in Table 1.

As an internal calibration standard the low-pressure absorption measurements were made with 0.25 Torr N_2O added to the cell (*20*). All scans were added and calibrated by linear regression with a single calibration factor. The emission measurements were calibrated internally by using the lower vibrational state transitions measured in absorption.

Calibration uncertainties (or errors) are difficult to estimate. For this paper we estimate that the calibration uncertainty should be given by the formula

$$\text{uncertainty (in cm}^{-1}) = \text{wavenumber} \times 2.0 \times 10^{-7}.$$

Those uncertainties primarily affect the vibrational energy levels given in the second columns of Tables 3 and 5 and should be added in quadrature to the uncertainties given in those tables.

For the emission measurements on $D^{12}C^{14}N$ the same quartz emission cell as described in Ref. (*18*) was used. For the emission measurements on $D^{13}C^{14}N$ a 90-cm cell made of Al_2O_3 was used. The cell was fitted with KBr windows that were kept at room temperature by water-cooled copper collars. The central 30 cm of the cell were placed in an oven that could be heated to 2000 K. The measurement itself took place at a temperature of about 1520 K.

For almost a hundred years it has been known that hydrogen cyanide decomposes when brought into contact with hot ceramic materials (*21*). To compensate for the slow decomposition of the sample, the contents of the cell were changed every 2 h. Each time the cell was filled to a pressure of about 12.5 mbar. The effect of pressure broadening was negligible compared to the high-temperature Doppler-broadening effect. At 1400 K the full Doppler width of the lines would be 0.0029 cm^{-1} at 570 cm^{-1} and 0.012 cm^{-1} at 2400 cm^{-1}. The effect of pressure shifting was neglected. The instrumental linewidth was roughly equal to the high-temperature Doppler width in each case.

The deuterium cyanide samples were prepared by treating potassium cyanide and phosphorus pentoxide with D_2O. In the case of preparing $D^{13}C^{14}N$ the potassium cyanide was enriched to 99% ^{13}C. The spectra all showed considerable contamination with HCN due to H_2O adsorbed on the surface of the emission cell. Later measurements on HCN showed similar contamination due to DCN, presumably arising from surface desorption. Some of the $D^{12}C^{14}N$ measurements made in the region 1800 to 2800 cm^{-1} came from DCN contamination found in the emission spectrum of HCN.

ANALYSIS OF THE MEASUREMENTS

Vibrational and Rotational Constants

The emission spectrum of $D^{13}C^{14}N$ is shown in Fig. 1. It is noticeable that the Q-branches are clustered according to the value of $v_2 - l$ with the highest-frequency cluster being the strongest.

Table 2 summarizes the various vibrational transitions that were observed in this work in either absorption or emission. Most of the rotational assignments were made with the help of the Giessen Loomis–Wood program (*22*). Unfortunately the l_{max} hot bands for $D^{13}C^{14}N$, beginning with $l = v_2 = 5$, overlap

TABLE 1
Parameters of the FTS Spectral Measurements Used in This Work

Filename	EDCNEAS	TGDCNAS	TGDCNDS	EDCNEES	TGDCNLU	TGDCNKU	EHCNEQS
Species	$D^{12}C^{14}N$	$D^{12}C^{14}N$	$D^{12}C^{14}N$	$D^{13}C^{14}N$	$D^{13}C^{14}N$	$D^{13}C^{14}N$	$H^{12}C^{14}N$
Region (cm^{-1})	400-877	400-720	900-1250	400-850	500-820	460-830	1800-7000
Date (D/M/Y)	4/2/97	19/1/95	18/10/95	29/7/97	26/9/97	25/9/97	21/1/97
Pressure (Torr)	4.2	3.3	4.09	12.1	0.24	1.5	22.8
Temperature (K)	1373	296.1	297.7	1523	300	300	1373
Pathlength (cm) total or of heated region	60	302	1968	30	338	338	60
Aperture diameter (mm)	3.15	1.7	1.5	3.15	1.7	1.7	2.5
Resolution (1/MOPD) (cm^{-1})	0.005	0.0019	0.0022	0.0072	0.0021	0.0021	0.0275
Scans coadded	680	324	400	550	69	60	1800
Detector	Ge:Cu (4K)	Ge:Cu(4K)	Ge:Cu(4K)	Ge:Cu(4K)	Ge:Cu(4K)	Ge:Cu(4K)	InSb
Windows	KBr	CsI	KBr	KBr	KBr	KBr	CaF_2
Beamsplitter	Mylar	Mylar	KBr	3.5 μm Mylar	3.5 μm Mylar	3.5 μm Mylar	Si:CaF_2
Focal length of collimator (mm)	418	418	418	418	418	418	418
Scanner velocity (cm/s)	1.266	1.266	1.266	1.266	1.266	1.266	1.266

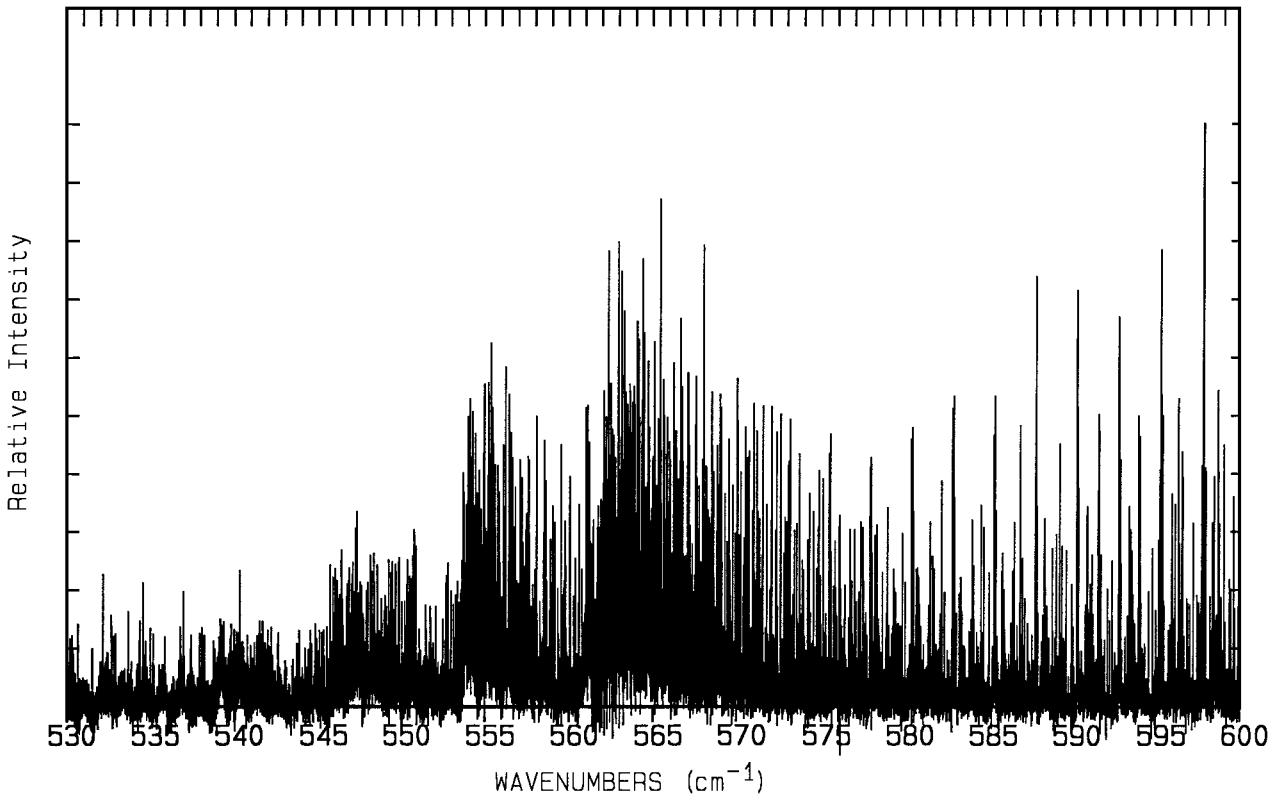

FIG. 1. Overview of the emission spectrum of the ν_2 region for $D^{13}C^{14}N$. The band center of the fundamental lies at 561.3 cm^{-1}. The Q-branches form clusters separated by about 7 cm^{-1}. The highest cluster, at about 561 cm^{-1}, has transitions with $\nu_2 - l = 0$, the next lower cluster has $\nu_2 - l = 2$, then $\nu_2 - l = 4$, etc.

almost exactly over a wide range of rotational quantum numbers, so the analysis of the l_{max} hot bands for that isotopomer becomes more difficult with increasing vibrational quantum number. Beginning with the seventh excited state it is impossible. On the other hand, the bands of the $l_{max} - 2$ series (for which $\nu_2 - l = 2$) are adjacent but nicely separated, so that an assignment was relatively easy. For $D^{12}C^{14}N$ the overlap of the l_{max} hot bands was not a problem and those transitions, which are generally the strongest transitions for a given value of ν_2, were identified up to $\nu_2 = 11 \rightarrow 10$.

The assignments were verified by the use of combination differences for the lower vibrational quantum numbers up to $\nu_2 = 3$ and by comparing the estimated values of the vibrational and rotational constants with those calculated at each step from the assigned lines. Additionally the relative line intensities, mostly given by the Hönl–London factors and the vibrational factor depending on ν_2 and l (*18*), were carefully regarded to verify the assignments.

The fitting program took into account the effects of l-type resonance by diagonalizing the Hamiltonian for each J value. The analysis used the following matrix elements:

$$\begin{aligned}\langle v, l, J|H|v, l, J\rangle &= G(v,l) + B_v[J(J+1) - l^2] - D_v[J(J+1) - l^2]^2 \\ &\quad + H_v[J(J+1) - l^2]^3 \qquad [1]\end{aligned}$$

$$\begin{aligned}\langle v, l, J|H|v, l \pm 2, J\rangle &= 1/4\{q_v - q_{vJ}J(J+1) + q_{vJJ}J^2(J+1)^2 + q_l(l \pm 1)^2\} \\ &\quad \times \{(\nu_2 \mp l)(\nu_2 \pm l + 2)[J(J+1) - l(l \pm 1)][J(J+1) \\ &\quad - (l \pm 1)(l \pm 2)]\}^{1/2} \qquad [2]\end{aligned}$$

$$\begin{aligned}\langle v, l, J|H|v, l \pm 4, J\rangle &= (\rho_v/16)\{(\nu_2 \mp l)(\nu_2 \pm l + 2)(\nu_2 \mp l - 2)(\nu_2 \pm l + 4) \\ &\quad \times [J(J+1) - l(l \pm 1)][J(J+1) - (l \pm 1)(l \pm 2)] \\ &\quad \times [J(J+1) - (l \pm 2)(l \pm 3)][J(J+1) \\ &\quad - (l \pm 3)(l \pm 4)]\}^{1/2}. \qquad [3]\end{aligned}$$

In Eq. [1] we use B_v, D_v, and H_v to indicate constants that actually depend on both v and l. Instead of reporting values of $G(v, l)$ it is more common to report values of $G_0(v, l) = G(v, l) - G(0, 0)$ to indicate vibrational energy levels that are measured relative to the ground vibrational state for which $v = 0$ and $l = 0$. Since the $G_0(v, l)$ do not always represent the center of the infrared bands, we also define a $G_c(v, l)$ that does define the band centers and may be determined from the equation

$$G_c(v, l) = G_0(v, l) - B_v l^2 - D_v l^4 - H_v l^6. \qquad [4]$$

TABLE 2
Band Centers in Wavenumbers (cm^{-1}) for the Infrared Bands Measured for This Work

transition	ν_c	transition	ν_c	transition	ν_c
$D^{13}C^{14}N$		$D^{12}C^{14}N$		$D^{12}C^{14}N$	
01^10-00^00	561.333 744(21)*†[a]	01^10-00^00	569.040 782(18)*†	08^60-07^50	560.560 9(12)*
02^00-00^00	1115.142 705(43)†	02^00-00^00	1129.988 301(25)†	08^80-07^70	567.931 24(50)*
02^00-01^10	553.808 96(4)*†	02^20-00^00	1137.891 564(22)†	09^70-08^60	560.474 0(11)*
02^20-01^10	561.207 82(3)*†	02^00-01^10	560.947 52(2)*†	09^90-08^80	567.817 67(53)*
03^10-02^00	553.795 16(6)*†	02^20-01^10	568.850 78(2)*†	010^80-09^70	560.383 02(79)*
03^10-02^20	546.396 30(7)*†	03^10-01^10	1121.848 08(2)†	$010^{10}0-09^90$	567.716 3(17)*
03^30-02^20	561.095 93(11)*†	03^30-01^10	1137.522 07(5)†	$011^{11}0-010^{10}0$	567.626 9(16)*
04^00-03^10	546.474 91(21)*	03^10-02^00	560.900 56(2)*†	00^01-00^00	1925.255 517(91)*†
04^20-03^10	553.780 33(24)*	03^10-02^20	552.997 30(2)*†	01^11-00^00	2497.135 49(14)*†
04^40-03^30	560.998 38(25)*	03^30-02^20	568.671 28(5)*†	01^11-01^10	1928.094 71(14)*†
05^10-04^00	546.538 07(28)*	04^00-02^00	1113.970 94(10)†	01^11-00^01	571.879 98(16)*
05^30-04^20	553.764 31(26)*	04^20-02^20	1113.843 66(12)†	02^01-02^00	1930.675 0(15)*
05^50-04^40	560.914 43(31)*	04^00-03^10	553.070 38(9)*†	02^21-02^20	1930.740 10(48)*
06^00-05^10	539.356 46(28)*	04^20-03^10	560.846 36(12)*†	02^01-01^11	563.527 8(16)*
06^20-05^10	546.586 07(51)*	04^40-03^30	568.502 39(15)*†	02^21-01^11	571.496 18(48)*
06^40-05^30	553.748 33(35)*	05^10-03^10	1106.189 93(17)†	00^02-00^01	1911.121 7(19)*
06^60-05^50	560.845 20(31)*	05^30-03^30	1105.957 20(28)†	10^00-00^00	2630.303 358(64)*†
07^10-06^00	539.450 87(36)*	05^10-04^00	553.119 55(18)*	11^10-01^10	2614.624 37(11)*†
07^30-06^20	546.613 5(27)*	05^10-04^20	545.343 57(19)*	12^00-02^00	2599.146 46(28)*
07^50-06^40	553.731 13(43)*	05^30-04^20	560.784 83(28)*	12^20-02^20	2598.995 31(41)*
08^00-07^10	532.351 9(57)*	05^50-04^40	568.343 56(23)*	13^10-03^10	2583.723 3(22)*
08^60-07^50	553.714 06(58)*	06^00-05^10	545.476 64(34)*	13^30-03^30	2583.402 2(27)*
09^70-08^60	553.697 88(60)*	06^20-05^10	553.146 40(56)*	14^20-04^20	2568.359(17)*
00^01-00^00	1911.841 522(46)†	06^40-05^30	560.716 41(34)*	14^40-04^40	2567.848 7(26)*
01^11-01^10	1913.813 9(31)†	06^60-05^50	568.195 55(26)*	20^00-00^00	5220.224 59(24)†
10^00-00^00	2590.066 81(17)†	07^10-06^00	545.571 59(45)*	20^00-10^00	2589.921 24(25)*
11^10-01^10	2575.240 3(11)†	07^30-06^20	553.148 98(115)*	21^10-01^10	5188.816 9(34)†
		07^50-06^40	560.641 81(47)*	10^01-00^00	4523.275 08(25)†
		07^70-06^60	568.057 47(42)*	10^01-00^01	2598.019 56(27)*
		08^00-07^10	538.044 5(39)*		

[a] The uncertainty in the last digits (twice the standard deviation) is given in parentheses. An asterisk,*, indicates the band was measured in emission and a dagger, †, indicates the band was measured in absorption.

These are the same matrix elements and constants as were used in an earlier paper on HCN emission measurements (*23*) and the same least-squares program was used in the present analysis. One feature of this program is that it treats the unresolved lines of split transitions as the average of the two split levels or transitions.

In the least-squares analyis data were drawn from other works (*13–18, 23, 26, 27*) and combined with the present data, with each set of data weighted by the inverse square of the measurement uncertainties. For some data, such as the millimeter-wave measurements, those uncertainties were taken from the literature. In other cases, the uncertainties were given by the rms (root-mean-square) deviation of each subband, or group of measurements. For the infrared data the uncertainties do not reflect calibration uncertainties, which were given in the section on experimental details. In general, the emission measurements were given uncertainties of 0.0005 cm^{-1}, except in the high-wavenumber region where the uncertainties were 0.002 cm^{-1}. The absorption measurements were given uncertainties of 0.0002 cm^{-1}.

Especially useful in the assignments were the R-branches of the rotation–vibration transitions. Due to the Hönl–London factors the intensities of the R-branch transitions are greater than those of the P-branch transitions, so that in many cases the R-branches are the only available information about the higher bending states. As mentioned before, the transitions in the R-branches of the l_{max} series of $D^{13}C^{14}N$ are severely overlapped, and therefore couldnot be used for many vibrational states. On the other hand, the transitions of the $l_{max} - 2$ series were nicely spread so that one could estimate the successive $l_{max} - 2$ series just by regarding the pattern of the previous $l_{max} - 2$ series in the Loomis–Wood plot. These difficulties were largely absent in $D^{12}C^{14}N$.

The molecular constants resulting from the fit of all assigned transitions are presented in Tables 3 to 6. Constants are included for several states which are not included in Table 2. These involve

data taken from earlier work (*13–18, 23, 26, 27*) and included in the present global fit.

Quantum Number Expansion of the Constants

After as many rotational–vibration lines as possible of each vibrational level were assigned, the molecular constants were fit to the usual series expansions in the vibrational quantum numbers. With the constants thus determined, we could predict the molecular constants of the next vibrational level. This process was begun using the constants given in Ref. (*18*) and, aside from a few additional constants, most of the constants were only changed by a small amount. The final constants obtained after all the measurements were added to the fit are given in Tables 7 to 9. In order to ensure that the constants for all isotopomers were based on comparable calculations, we refit the constants for $D^{12}C^{15}N$ and $D^{13}C^{15}N$ and show those revised constants as well. Since most of the constants were only marginally changed upon isotopic substitution, if a constant could not be determined for one isotopomer, that constant was fixed at the value found for $D^{12}C^{14}N$, except for the constants calculated by Nakagawa and Morino (*24*). Instead of transferring directly the constants found for $D^{12}C^{14}N$, we used, for the x_{ij} constants, the ratio given by the calculations of Nakagawa and Morino. For those constants that could be determined for two or more isotopomers, the substitution ratio observed was found to be very close to that given by Nakagawa and Morino (*24, 25*).

TABLE 3
Rovibrational Constants for $D^{12}C^{14}N$ in cm^{-1} after Correction for *l*-Type Resonance

$v_1 v_2\ l\ v_3$	$G_0(v,l)$[a]	B_v	$D_v \times 10^6$	$H_v \times 10^{12}$	J_{max}
0 0 0 0	0.0	1.207 750 950(16)[b]	1.926 84(18)	2.773(75)	65
0 1 1 0	570.252 855(18)	1.212 072 630(41)	1.996 67(19)	3.572(73)	69
0 2 0 0	1129.988 301(25)	1.216 649 344(84)	2.066 16(22)	4.807(83)	62
0 2 2 0	1142.756 661(22)	1.216 274 045(62)	2.068 16(19)	4.218(72)	62
0 3 1 0	1692.109 974(25)	1.221 113 751(78)	2.137 76(86)	5.909(77)	58
0 3 3 0	1717.545 947(49)	1.220 344 308(164)	2.140 27(84)	4.498(84)	59
0 4 0 0	2243.959 237(96)	1.225 849 161(828)	2.209 3(22)	7.62(48)	58
0 4 2 0	2256.637 039(118)	1.225 454 473(644)	2.209 6(12)	6.69(31)	57
0 4 4 0	2294.653 574(145)	1.224 271 259(739)	2.211 8(18)	3.88(36)	50
0 5 1 0	2798.309 263(169)	1.230 471 011(964)	2.282 1(29)	8.37(65)	58
0 5 3 0	2823.586 989(267)	1.229 659 49(128)	2.278 4(16)	5.88(48)	57
0 5 5 0	2874.109 953(248)	1.228 046 37(125)	2.288 1(32)	4.95(60)	51
0 6 0 0	3342.555 433(372)	1.235 383 37(236)	2.361 5(38)	[9.35][c]	55
0 6 2 0	3355.165 061(555)	1.234 966 27(206)	2.353 3(32)	[8.67]	44
0 6 4 0	3392.975 993(388)	1.233 720 55(159)	2.351 7(13)	[6.62]	43
0 6 6 0	3455.943 916(325)	1.231 654 78(174)	2.363 7(48)	5.30(81)	48
0 7 1 0	3889.367 202(548)	1.240 180 83(441)	2.456 0(92)	[10.29]	54
0 7 3 0	3914.528 12(125)	1.239 327 43(786)	2.422 6(124)	[8.92]	23
0 7 5 0	3964.819 00(57)	1.237 628 69(309)	2.431 6(41)	[6.19]	31
0 7 7 0	4040.181 09(46)	1.235 087 26(213)	2.440 1(69)	[2.09]	41
0 8 0 0	4426.171 49(401)	1.245 330 9(381)	2.550(24)	[11.57]	37
0 8 2 0	[4438.727 55]	[1.244 835 3]	[2.497 9]	[10.89]	
0 8 4 0	[4476.396 56]	[1.243 532 8]	[2.500 0]	[8.84]	
0 8 6 0	4539.128 01(112)	1.241 356 9(65)	2.500 3(104)	[5.42]	30
0 8 8 0	4626.845 83(60)	1.238 324 6(23)	2.516 2(106)	[0.63]	42
0 9 1 0	[4965.543 89]	1.250 245 8(80)	[2.570 9]	[12.51]	21[d]
0 9 3 0	[4990.630 79]	[1.249 357 4]	[2.572 0]	[11.14]	
0 9 5 0	[5040.774 37]	[1.247 578 8]	[2.574 1]	[8.41]	
0 9 7 0	5115.913 70(138)	1.244 908 1(88)	2.572 8(116)	[4.3]	30
0 9 9 0	5215.960 04(73)	1.241 349 6(28)	2.583 1(123)	[−1.17]	41
0 10 0 0	[5494.941 17]	[1.255 546 7]	[2.644 9]	[13.79]	
0 10 2 0	[5507.475 37]	[1.255 091 4]	[2.645 3]	[13.11]	
0 10 4 0	[5545.062 87]	[1.253 725 4]	[2.646 4]	[11.06]	
0 10 6 0	[5607.658 32]	[1.251 448 9]	[2.648 2]	[7.64]	
0 10 8 0	5695.184 45(152)	1.248 253 5(92)	2.640 6(123)	[2.85]	31
0 10 10 0	5807.541 85(118)	1.244 148 6(87)	2.642 1(210)	[−3.30]	25

[a] To get observed band center use $G_c(v,l) = G_0(v,l) - B_v l^2 - D_v l^4 - H_v l^6$.
[b] The uncertainty in the last digits, twice the estimated standard error, is given in parentheses.
[c] Constants enclosed in square brackets were fixed for the last-squares fit.
[d] Laser measurements provide the only direct information on the 02^02 and 09^10 levels.

TABLE 3—*Continued*

v_1v_2	l	v_3	$G_0(v,l)$[a]	B_v	$D_v\times10^6$	$H_v\times10^{12}$	J_{max}
0 11	1	0	[6026.884 93]	[1.260 723 1]	[2.719 6]	[14.73]	
0 11	3	0	[6051.936 82]	[1.259 790 8]	[2.720 0]	[13.36]	
0 11	5	0	[6102.010 35]	[1.257 926 1]	[2.720 9]	[10.63]	
0 11	7	0	[6177.045 06]	[1.255 129 1]	[2.722 1]	[6.52]	
0 11	9	0	[6276.950 27]	[1.251 399 7]	[2.723 8]	[1.05]	
0 11	11	0	6401.606 26(144)	1.246 713 5(106)	2.707 4(257)	[−5.78]	26
0 0	0	1	1925.255 517(91)	1.201 206 746(167)	1.925 57(62)	2.96(34)	50
0 1	1	1	2498.340 811(136)	1.205 318 528(1022)	1.996 1(19)	3.15(88)	46
1 0	0	0	2630.303 358(64)	1.197 415 014(317)	1.909 69(39)	3.03(11)	65
0 2	0	1	3060.663 34(155)	1.209 673 5(65)	2.068 4(53)	[5.17]	40
0 2	2	1	3073.468 756(474)	1.209 272 0(19)	2.072 7(14)	[4.48]	37
1 1	1	0	3184.867 182(111)	1.202 029 050(483)	1.977 71(55)	4.15(13)	70
0 3	1	1	3625.17(5)				
1 2	0	0	3729.134 760(285)	1.206 912 36(192)	2.043 1(13)	[5.32]	43
1 2	2	0	3741.713 216(403)	1.206 585 63(226)	2.039 5(21)	3.78(51)	60
0 0	0	2	3836.377 21(194)	1.194 652 8(81)	1.923 4(60)	[3.20]	37
1 3	1	0	4275.823 92(216)	1.211 762 7(92)	2.115 5(80)	[6.26]	43
1 3	3	0	4300.865 33(267)	1.211 144 4(109)	2.114 7(92)	[4.89]	40
0 1	1	2	4412.175 11(155)	1.198 535 0(117)	2.011(17)	[4.14]	27
1 0	0	1	4523.275 077(251)	1.191 145 412(1598)	1.896 8(12)	[3.35]	49
1 4	0	0	[4812.456 18]	[1.216 804]	[2.178 8]	[7.54]	
1 4	2	0	4824.960 3(168)	1.216 469 9(367)	[2.180 0]	[6.85]	27
1 4	4	0	4862.365 64(248)	1.215 732 6(65)	[2.184]	[4.80]	28
0 2	2	0	4977.045 3(31)	1.202 348 2(52)	[2.074 3]	[5.42]	23[d]
0 2	2	2	[4989.887 41]	[1.201 921 7]	[2.075 9]	[4.74]	
1 1	1	1	5080.659 8(47)	1.195 688(56)	1.996(136)	[4.29]	19
2 0	0	0	5220.224 593(239)	1.187 047 413(1508)	1.896 87(190)	[3.51]	38
2 1	1	0	5759.049 620(3372)	1.191 960 86(4829)	2.003(147)	[4.46]	16

TABLE 4
***l*-Type Resonance Constants for $D^{12}C^{14}N$ in cm^{-1}**

$v_1v_2v_3$	$q_0\times10^3$	$q_{vJ}\times10^8$	$q_{vJJ}\times10^{12}$	$\rho_v\times10^8$
0 1 0	6.210 657 3(8)[a]	7.344 3(8)	1.421(9)	
0 2 0	6.288 501(32)	7.732 7(70)	1.575(28)[b]	[-1.260][c]
0 3 0	6.368 248(23)	8.143 2(60)	1.728(25)	-1.275(54)
0 4 0	6.450 019(245)	8.555(38)	1.881(139)	-1.313(56)
0 5 0	6.534 40(15)	9.021(37)	1.913(184)	-1.338(57)
0 6 0	6.621 13(44)	9.607(42)	[2.17]	-1.338(57)
0 7 0	6.708 43(76)	10.35(19)	2.46(23)	-1.217(72)
0 8 0	6.800 7(74)	[10.66]	[2.48]	[-1.34]
0 9 0	[6.891 8]	[11.25]	[2.63]	[-1.34]
010 0	[6.986 5]	[11.88]	[2.78]	[-1.34]
011 0	[7.083 3]	[12.53]	[2.93]	[-1.34]
0 1 1	6.388 29(64)	6.337(61)	[1.42]	
0 2 1	6.485 89(254)	6.55(27)	[1.57]	[-1.260]
1 1 0	6.049 42(64)	8.536(87)	1.64(20)	
1 2 0	6.103 30(223)	8.991(120)	[1.79]	[-1.260]
1 3 0	6.168 7(58)	11.92(65)	[1.89]	[-1.260]
1 4 0	[6.222 5]	[9.84]	[2.02]	[-1.260]
1 1 1	6.145 5(127)	[7.58]	[1.64]	
0 1 2	6.655 4(71)	[5.31]	[1.42]	
0 2 2	[6.773 1]	[5.70]	[1.58]	[-1.260]
2 1 0	5.900 7(107)	[9.84]	[1.86]	

[a] The uncertainty in the least digits, twice the estimated standard deviation, is given in parentheses.

[b] For $v_2 > 1$ the data were fit with $q_l = (0.427 \pm 0.032) \times 10^{-5}\ cm^{-1}$.

[c] Values enclosed in square brackets were fixed in the least-squares fit.

The constants given in Table 7 were determined by the use of the following expansion:

$$\begin{aligned} G(v,l) = &\sum \omega_i(v_i + d_i/2) \\ &+ \sum\sum x_{ij}(v_i + d_i/2)(v_j + d_j/2) + g_{22}l^2 \\ &+ \sum\sum\sum y_{ijk}(v_i + d_i/2)(v_j + d_j/2)(v_k + d_k/2) \\ &+ \sum y_{ill}(v_i + d_i/2)l^2 + \sum\sum\sum\sum z_{ijkh} \\ &\times (v_i + d_i/2)(v_j + d_j/2)(v_k + d_k/2)(v_h + d_h/2) \\ &+ \sum\sum z_{ijll}(v_i + d_i/2)(v_j + d_j/2)l^2 + z_{llll}l^4 \\ &+ z_{22222}(v_2+1)^5 + z_{222ll}(v_2+1)^3l^2 + z_{2llll}(v_2+1)l^4. \end{aligned} \quad [5]$$

Here and in the following equations the sums run over 1, 2, and 3 for the three normal vibrational modes with the condition that $h \geq k \geq j \geq i$. The degeneracy of the normal modes, d, is 1 for the stretching modes and 2 for the bending mode. Not all the terms in Eq. [5] could be determined even for $D^{12}C^{14}N$ for which we have the most data.

The rotational constants and the centrifugal distortion constants given in Tables 8 and 9 were determined through the

TABLE 5
Rovibrational Constants for $D^{13}C^{14}N$ in cm^{-1} after Correction for *l*-Type Resonance

$v_1v_2l\,v_3$	$G_0(v,l)$[a]	B_v	$D_v\times10^6$	$H_v\times10^{12}$	J_{max}
0 0 0 0	0.0	1.187 076 253(61)[b]	1.855 20(46)	2.57(24)	65
0 1 1 0	562.524 803(21)	1.191 059 163(46)	1.918 22(45)	3.23(23)	68
0 2 0 0	1115.142 705(43)	1.195 292 715(100)	1.980 11(44)	4.25(22)	68
0 2 2 0	1127.321 246(37)	1.194 919 346(73)	1.982 82(44)	3.72(22)	68
0 3 1 0	1670.137 277(70)	1.199 410 754(227)	2.043 99(48)	5.10(21)	61
0 3 3 0	1694.425 317(109)	1.198 645 945(412)	2.047 93(55)	3.92(22)	60
0 4 0 0	2215.412 774(219)	1.203 793 90(129)	2.106 70(170)	5.73(45)	62
0 4 2 0	2227.531 806(250)	1.203 403 172(956)	2.108 78(104)	5.83(33)	56
0 4 4 0	2263.871 528(261)	1.202 227 55(107)	2.112 98(118)	3.58(36)	51
0 5 1 0	2763.158 906(320)	1.208 061 09(174)	2.171 64(216)	7.10(78)	58
0 5 3 0	2787.347 835(346)	1.207 258 67(154)	2.174 62(171)	6.39(56)	54
0 5 5 0	2835.691 646(377)	1.205 653 07(145)	2.177 07(159)	2.29(52)	52
0 6 0 0	3301.307 303(401)	1.212 611 83(204)	2.237 96(298)	[7.54][c]	59
0 6 2 0	3313.385 717(537)	1.212 199 38(200)	2.234 46(152)	[7.00]	48
0 6 4 0	3349.606 245(445)	1.210 963 14(173)	2.237 04(146)	[5.39]	42
0 6 6 0	3409.916 392(417)	1.208 913 02(124)	2.245 39(78)	[2.71]	48
0 7 1 0	3841.975 22(52)	1.217 050 80(384)	2.322 7(70)	[8.28]	51
0 7 3 0	3866.096 36(272)	1.216 214 5(84)	2.306 2(56)	[7.21]	32
0 7 5 0	3914.324 66(60)	1.214 507 9(29)	2.297 2(35)	[5.06]	34
0 7 7 0	[3986.573 98]	[1.211 985 5]	[2.311]	[1.84]	
0 8 0 0	4373.110 09(572)	1.221 777 0(404)	2.368 1(467)	[9.29]	45
0 8 2 0	[4385.162 17]	[1.221 339 3]	[2.36]	[8.75]	
0 8 4 0	[4421.317 09]	[1.220 044 5]	[2.366]	[7.14]	
0 8 6 0	4481.519 79(77)	1.217 882 6(45)	2.364 9(135)	[4.46]	34
0 8 8 0	[4565.687 51]	[1.214 865 4]	[2.379]	[7.10]	
0 9 1 0	[4906.764 19]	[1.226 376 1]	[2.427]	[10.81]	
0 9 3 0	[4930.865 57]	[1.225 492 1]	[2.429]	[9.45]	
0 9 5 0	[4979.035 09]	[1.223 724 0]	[2.433]	[6.72]	
0 9 7 0	5051.206 39(89)	1.221 071 2(52)	2.430 8(71)	[2.64]	26
0 9 9 0	[5147.279 51]	[1.217 535 8]	[2.448]	[−2.81]	
0 0 0 1	1911.841 522(46)	1.180 668 233(412)	1.855 76(69)	[2.37]	26
0 1 1 1	2476.332 16(308)	1.184 468 6(562)	2.059(206)	[3.06]	16
1 0 0 0	2590.066 809(174)	1.177 370 26(129)	1.837 99(169)	[2.37]	29
1 1 1 0	3137.755 68(108)	1.181 632 97(1122)	1.886 3(220)	[3.06]	21

[a] To get observed band center use $G_c(v,l) = G_0(v,l) - B_v l^2 - D_v l^4 - H_v l^6$.
[b] The uncertainty in the last digits, twice the estimated standard error, is given in parentheses.
[c] Constants enclosed in square brackets were fixed for the least-squares fit.

following expansion series:

$$B_v = B_e - \sum \alpha_i (v_i + d_i/2) + \sum\sum \gamma_{ij}(v_i + d_i/2)(v_j + d_j/2) + \gamma_{ll} l^2 + \sum\sum\sum \gamma_{ijk}(v_i + d_i/2)(v_j + d_j/2)(v_k + d_k/2) + \sum \gamma_{ill}(v_i + d_i/2) l^2 + \gamma_{2233}(v_2 + 1)^2 (v_3 + 1/2)^2 + \gamma_{12ll}(v_1 + 1/2)(v_2 + 1) l^2 + \gamma_{22ll}(v_2 + 1)^2 l^2, \quad [6]$$

$$D_v = D_e + \sum \beta_i (v_i + d_i/2) + \beta_{ll} l^2 + \beta_{2ll}(v_2 + 1) l^2, \quad [7]$$

and

$$H_v = H_e + \sum \epsilon_i (v_i + d_i/2) + \epsilon_{ll} l^2. \quad [8]$$

For the *l*-type resonance constants in Table 9 the following expansions were used:

$$q_v = q_e + \sum \pi_i (v_i + d_i/2) + \sum\sum \pi_{ij}(v_i + d_i/2)(v_j + d_j/2), \quad [9]$$

$$q_{vJ} = q_{eJ} + \sum \pi_{iJ}(v_i + d_i/2) + \pi_{22J}(v_2 + 1)^2, \quad [10]$$

$$q_{vJJ} = q^*_{JJ} + \pi_{1JJ}(v_1 + 1/2) + \pi_{2JJ}(v_2 + 1), \quad [11]$$

and

$$\rho_v = \rho^* + \rho_2 (v_2 + 1). \quad [12]$$

Analyzing the Laser Transitions

Although transitions from the highest *l* values of the $v_2 = 9$ state were observed in the emission spectrum, the weaker

TABLE 6
***l*-Type Resonance Constants for $D^{13}C^{14}N$ in cm^{-1}**

$v_1v_2v_3$	$q_v \times 10^3$	$q_{vJ} \times 10^8$	$q_{vJJ} \times 10^{12}$	$\rho_v \times 10^8$
0 1 0	6.080 680 3(91)[a]	6.928 0(27)	1.262(23)	
0 2 0	6.155 665(150)	7.268 2(146)	1.345(40)[b]	[−1.26][c]
0 3 0	6.232 279(179)	7.635 6(193)	1.458(50)	−1.266(3)
0 4 0	6.310 629(312)	7.990(45)	1.418(134)	−1.277(11)
0 5 0	6.392 00(42)	8.517(60)	2.024(215)	−1.323(10)
0 6 0	6.474 71(30)	8.920(37)	[1.78]	−1.347(18)
0 7 0	6.560 53(91)	9.789(138)	[1.88]	−1.353(39)
0 8 0	6.647 0(76)	9.817(328)	[1.99]	[−1.39]
0 9 0	[6.736]	[9.99]	[2.09]	[−1.42]
0 1 1	6.285 3(163)	[6.92]	[1.26]	
1 1 0	5.911 89(296)	[6.92]	[1.18]	

[a] The uncertainty in the last digits, twice the estimated standard deviation, is given in parentheses.
[b] For $v_2 > 1$ the data were fit with q_l fixed at 0.40×10^{-5} cm^{-1}.
[c] Values enclosed in square brackets were fixed in the least-squares fit.

transitions to the 09^10 level could not be identified. After the constants in the power series expansion had been determined without including the $D^{12}C^{14}N$ laser transition measurements, we calculated the laser transitions to verify that they have been correctly identified. The agreement between the calculated and observed laser transitions was within ± 0.0001 cm^{-1} for the purely rotational transitions. The separation of the $J = 21$ levels of the 02^02 and $09^{1e}0$ states was calculated to be 0.06 cm^{-1} which was greater than the observed separation, 0.01 cm^{-1}, but in good agreement considering that neither of the two vibrational states had been directly observed by us. The five c.w. laser transitions measured by Hocker and Javan (*26*) with an accuracy of ± 3 MHz (± 0.0001 cm^{-1}) and the one other pulsed laser transition (*27*) measured with considerably less accuracy (± 0.004 cm^{-1}) were then added to the fit after correcting for the effect of the Coriolis coupling of the two states.

The correction for the perturbation was made by assuming that the calculated separation of the $J = 21$, $J = 20$ levels of $09^{1e}0$ is correct in the absence of the perturbation. The difference between the observed and calculated separation represents the displacement of the $J = 21$ level. This shows that the $J = 21$ level is displaced to lower wavenumbers by 0.00558 cm^{-1}. The $J = 21$ level of the 02^02 state will then be displaced to higher wavenumbers by the same amount. The observed separation of the two levels, Δ, is 0.0163 cm^{-1}, according to the measured laser transitions. The unperturbed separation of the two $J = 21$ levels, δ, will then be $0.0163 - 2(0.00558) = 0.005145$ cm^{-1}.

TABLE 7
Constants in cm^{-1} for the Vibrational Energy Levels of Four Isotopomers of DCN

Parameter	$D^{12}C^{14}N$	$D^{13}C^{14}N$	$D^{12}C^{15}N$	$D^{13}C^{15}N$
ω_1	2702.548 57(309)[a]	2660.874 75(106)	2693.487 96(50)	2652.573 55(135)
ω_2	579.663 95(379)	571.593 72(170)	578.328 00(87)	570.222 66(125)
ω_3	1952.281 17(773)	1938.615 21(298)	1925.988 08(102)	1911.012 87(58)
x_{11}	−20.166 21(148)	[−20.40][b]	[−20.63]	[−20.88]
x_{22}	−2.145 63(108)	−1.967 654(439)	−2.174 218(326)	−1.989 603(581)
x_{33}	−6.966 84(377)	[−6.93]	[−6.81]	[−6.77]
x_{12}	−15.785 31(311)	−14.933 94(102)	−15.668 288(425)	−14.804 08(129)
x_{13}	−32.283 84(24)	[−30.18]	[−30.79]	[−28.78]
x_{23}	3.403 67(937)	2.526 16(298)	3.477 254(1018)	2.589 881(529)
g_{22}	3.255 652(297)	3.094 542(230)	3.291 266(35)	3.132 852(187)
y_{222}	0.025 484(73)	0.020 538(141)	0.025 751(48)	0.021 575(153)
y_{112}	−0.024 86(147)	[−0.024]	[−0.024]	[−0.023]
y_{122}	0.064 15(23)	[0.064]	[0.063]	[0.062]
y_{223}	−0.153 57(271)	[−0.15]	[−0.15]	[−0.15]
y_{233}	−0.120 16(449)	[−0.12]	[−0.12]	[−0.12]
y_{1ll}	−0.044 50(44)	[−0.044]	[−0.044]	[−0.044]
y_{2ll}	−0.017 193(81)	−0.012 284(139)	[−0.016]	−0.013 342(92)
y_{3ll}	0.009 266(351)	[0.009 2]	[0.009]	[0.009 2]
z_{2222}	−0.000 844 0(106)	−0.000 688(20)	[−0.000 7]	−0.000 740 1(183)
z_{2233}	0.020 08(125)	[0.020 08]	[0.020 08]	[0.020 08]
z_{22ll}	0.000 872 4(118)	0.000 719(26)	[0.000 75]	0.000 804 8(143)
z_{12ll}	−0.001 001(126)	[−0.001]	[−0.001]	[−0.001]
z_{llll}	−0.000 104 4(32)	−0.000 111 4(11)	[−0.000 09]	−0.000 117 37(135)
z_{22222}	0.000 008 30(56)	0.000 004 9(11)	[0.000 006]	0.000 007 04(81)
z_{222ll}	−0.000 012 63(89)	−0.000 008 0(16)	[−0.000 012]	−0.000 011 94(76)
z_{2llll}	0.000 003 32(40)	[0.000 003 3]	[0.000 003 3]	[0.000 003 3]
std. dev. of fit	1.7[c]	1.9	2.5	3.6
Number of non-zero weighted measurements:	47	25	9	33

[a] The uncertainty (one standard deviation) in the last digits is given in parentheses.
[b] Values enclosed in square brackets were fixed during the fit.
[c] Since the standard deviations come from weighted fits, they are dimensionless.

TABLE 8
Rotational Constants in $cm^{-1} \times 10^{-3}$ for Four Isotopomers of DCN

Parameter	$D^{12}C^{14}N$	$D^{13}C^{14}N$	$D^{12}C^{15}N$	$D^{13}C^{15}N$
B_e	1211.838 57(2625)	1191.126 3(393)[a]	1177.071 34(453)	1155.722 81(956)
B_0	1207.750 948(23)	1187.076 230(84)	1173.138 248(3)	1151.840 212(137)
α_1	10.709 1(65)	10.058 7(158)	10.309 55(444)	9.667 0(159)
α_2	−4.428 2(328)	−4.074 6(393)	−4.266 72(448)	−3.941 88(950)
α_3	6.213 1(689)	6.109 8(770)	5.988 98(788)	5.867 55(1050)
γ_{11}	−0.015 86(121)	[−0.016][b]	[−0.016]	[−0.016]
γ_{22}	−0.023 18(881)	−0.021 23(23)	−0.021 218(75)	−0.022 726(275)
γ_{33}	−0.145 0(337)	[−0.144]	[−0.144]	[−0.144]
γ_{12}	0.256 54(725)	0.243 7(155)	0.224 86(422)	0.203 13(1575)
γ_{13}	0.274 69(241)	[0.26]	[0.26]	[0.26]
γ_{23}	−0.596 3(857)	−0.542 2(770)	−0.543 5(79)	−0.532 1(105)
γ_{ll}	−0.075 53(220)	−0.075 625(221)	−0.072 170(193)	−0.071 941(206)
γ_{222}	0.000 597(15)	0.000 557(23)	[0.000 5]	0.000 470 7(319)
γ_{122}	0.010 98(184)	[0.011]	[0.011]	[0.011]
γ_{223}	0.137 6(228)	[0.13]	[0.13]	[0.13]
γ_{233}	0.215 2(414)	[0.21]	[0.21]	[0.21]
γ_{1ll}	−0.016 70(358)	[−0.016]	[−0.016]	[−0.016]
γ_{2ll}	−0.006 983(456)	−0.006 837(93)	−0.006 837(59)	−0.006 758(70)
γ_{3ll}	−0.006 54(252)	[−0.006 4]	[−0.006 4]	[−0.006 4]
z_{2233}	−0.075 03(1066)	[−0.074]	[−0.074]	[−0.074]
z_{12ll}	0.009 657(905)	[0.009 5]	[0.009 5]	[0.009 5]
z_{22ll}	−0.000 025 2(36)	−0.000 027(9)	[−0.000 023]	−0.000 018 9(51)
std. dev. of fit:	2.9[c]	2.7	2.1	4.4
number of non-zero weighted measurements:	48	26	10	34

[a] The uncertainty (one standard deviation) in the last digits is given in parentheses.
[b] Values enclosed in square brackets were fixed during the fit.
[c] Since the standard deviations come from weighted fits, they are dimensionless.

If W is the off-diagonal coupling constant connecting the two levels then

$$\Delta^2 = 4W^2 + \delta^2. \quad [13]$$

We find that $W = 0.00774\ cm^{-1}$, about the order of magnitude expected. With such a coupling constant, the $J = 20$ and $J = 22$ levels should be shifted by only $0.000054\ cm^{-1}$.

DISCUSSION

The bending vibrations of $D^{12}C^{14}N$ and $D^{13}C^{14}N$ have been observed to the ninth excited state and even to $v_2 = 11$ for the former isotopomer. As was seen in previous measurements, the potential function for the bending motion is fairly harmonic so that the predictions of each successive higher vibrational level were reliable. As earlier observed, the constants change only slightly from one isotopomer to another for heavy atom substitutions, provided the data are analyzed in a consistent manner. The main difference between the present constants and those given earlier (*18*) is due to the need for a few higher order constants because of the more extensive measurements for DCN. Comparison with the earlier work shows the sensitivity of the constants to the inclusion of more constants and therefore the importance of making a consistent analysis for all isotopomers.

The present measurements give a value for the l-dependent l-type resonance constant, q_l, that is slightly smaller, but similar in magnitude and sign to the values found for some HCN isotopomers (*23*). Since there is a strong correlation between q_l and ρ, the present new values for ρ are quite different from the values given in earlier work (*18*) where q_l was not determinable. Only in the case of the more extensive measurements on $D^{12}C^{14}N$ could we simultaneously determine a value for ρ and q_l, consequently the same value of q_l was assumed for the other isotopomers of DCN in order to obtain a consistent analysis for all the isotopomers.

In addition to the interaction between the nearby $09^{1e}0$ and 02^02 levels of $D^{12}C^{14}N$ we have also found that the 10^01 and $08^{6e}0$ levels of $D^{13}C^{15}N$ cross at $J = 14$. Transitions involving the $08^{6e}0$ $J = 14$ level are not fit well, but otherwise do not seem to show the effect of what should be a very weak interaction because of the large Δl involved. However, we have noticed that the D_v for the 08^60 state is too small; see Table 2 of Ref. (*18*). Centrifugal distortion constants can be a sensitive indicator of some perturbations but it is not certain that the perturbation and the small value for D_v are related.

We have also found that the 01^12 level of $D^{13}C^{14}N$ is only about 1.5 cm^{-1} above the 08^00 level, so they should cross between $J = 5$ and $J = 6$ but the interaction at such low J should be hard to detect. Our measurements on the 08^00 level only go down to $J = 16$. The 02^02 level is about

TABLE 9
Some Higher Order Constants in cm^{-1}

Parameter	$D^{12}C^{14}N$	$D^{13}C^{14}N$	$D^{13}C^{15}N$
$D_e \times 10^6$	1.863 65(136)[a]	1.798 06(132)	1.690 02(245)
$\beta_1 \times 10^7$	−0.075(15)	−0.081(20)	−0.068(21)
$\beta_2 \times 10^7$	0.688(8)	0.623(5)	0.576(12)
$\beta_3 \times 10^7$	0.020(21)	0.039(9)	0.029(29)
$\beta_{22} \times 10^7$	0.002 8(8)	0.001 4(6)	0.001 2(22)
$\beta_{12} \times 10^7$	−0.031 5(63)	[−0.031][b]	[−0.031]
$\beta_{13} \times 10^7$	−0.120(19)	[−0.120]	[−0.120]
$\beta_{23} \times 10^7$	0.027(10)	[0.027]	[0.027]
$\beta_{ll} \times 10^7$	0.006 2(13)	0.007 1(4)	0.008 1(16)
$\beta_{2ll} \times 10^7$	−0.000 60(21)	[−0.000 60]	[−0.000 60]
std. dev.	2.6[c]	2.3	7.1
# of measurements	44	26	34
$H^* \times 10^{12}$	1.408(78)	1.374(54)	0.890(77)
$\xi_1 \times 10^{12}$	0.38(11)	[0.38]	[0.38]
$\xi_2 \times 10^{12}$	1.105(38)	0.937(54)	0.740(77)
$\xi_{ll} \times 10^{12}$	−0.171(13)	−0.167(15)	−0.085(32)
std. dev.	2.4	1.5	1.4
# of measurements	17	12	6
$q_e \times 10^3$	6.069 2(61)	5.935 4(82)	5.608 9(107)
$\pi_1 \times 10^4$	−0.89(12)	−0.969(29)	−0.536(37)
$\pi_2 \times 10^4$	0.735(14)	0.707 7(21)	0.665 7(54)
$\pi_3 \times 10^4$	0.89(10)	1.15(16)	0.59(21)
$\pi_{11} \times 10^4$	0.063(47)	[0.063]	[0.062]
$\pi_{22} \times 10^4$	0.010 69(13)	0.010 05(26)	0.009 22(84)
$\pi_{33} \times 10^4$	0.448(32)	[0.45]	[0.43]
$\pi_{12} \times 10^4$	−0.221(16)	[−0.22]	[−0.21]
$\pi_{13} \times 10^4$	−0.81(11)	[−0.81]	[−0.80]
$\pi_{23} \times 10^4$	0.199(23)	[0.20]	[0.19]
std. dev.	1.7	2.0	4.5
# of measurements	16	10	9
$q_J^* \times 10^8$	6.554(84)	6.215(6)	5.660(6)
$\pi_{1J} \times 10^8$	1.25(12)	[1.24]	[1.2]
$\pi_{2J} \times 10^8$	0.306(26)	0.266(6)	0.246(6)
$\pi_{3J} \times 10^8$	−1.02(11)	[−1.00]	[−1.00]
$\pi_{22J} \times 10^8$	0.016(4)	[0.015]	[0.014]
std. dev.	3.5	2.5	1.3
# of measurements	12	8	7
$q_{JJ}^* \times 10^{12}$	1.004(45)	0.952(27)	0.873(44)
$\pi_{1JJ} \times 10^{12}$	0.216(89)	[0.20]	[0.20]
$\pi_{2JJ} \times 10^{12}$	0.154(7)	0.103(27)	0.066(44)
std. dev.	0.9	2.4	1.7
# of measurements	7	5	4
$\rho^* \times 10^8$	−1.150(4)	−1.163(3)	
$\rho_2 \times 10^8$	−0.032(4)	−0.026(3)	
std. dev.	0.2	1.8	
# of measurements	3	5	

[a] The uncertainty in the last digits, one standard deviation, is given in parentheses.

[b] Constants enclosed in square brackets were fixed for the least-squares fit.

[c] The standard deviations are dimensionless because they come from weighted fits.

25 cm^{-1} above the $09^{1e}0$ level and the 02^22 and 09^30 levels are even closer but those vibrational states have not been observed.

The new values for B_e are consistently smaller than the values used in Ref. (*23*) by about 1.9 MHz. They give a CH internuclear distance that is larger by about 0.0002×10^{-8} cm and a CN internuclear distance that is shorter by 0.00006×10^{-8} cm.

ACKNOWLEDGMENTS

The authors thank Dr. S. Klee, Dr. M. Lock, Dipl.-Chem. M. Jung, and Dipl.-Ing. G. Mellau, who helped in constructing the emission apparatus and with the measurements.

REFERENCES

1. X. Yang, C. A. Rogaski, and A. M. Wodtke, *J. Opt. Soc. Am. B* **7,** 1835–1850 (1990).
2. P. R. Bunker and D. J. Howe, *J. Mol. Spectrosc.* **83,** 288–303 (1980).
3. J. N. Murrel, S. Carter, and L. O. Halonen, *J. Mol. Spectrosc.* **93,** 307–316 (1982).
4. F. Gatti, Y. Justum, M. Menou, A. Nauts, and X. Chapuisat, *J. Mol. Spectrosc.* **181,** 403–423 (1997).
5. A. G. Maki, *J. Mol. Spectrosc.* **58,** 308–315 (1975).
6. J.-I. Choe, D. K. Kwak, and S. G. Kukolich, *J. Mol. Spectrosc.* **121,** 75–83 (1987).
7. A. G. Maki, W. Quapp, S. Klee, G. C. Mellau, and S. Albert, *J. Mol. Spectrosc.* **180,** 323–336 (1996).
8. M. J. Winter and W. J. Jones, *J. Chem. Soc. Faraday Trans. 2* **78,** 585–594 (1982).
9. J. B. Burkholder, A. Sinha, P. D. Hammer, and C. J. Howard, *J. Mol. Spectrosc.* **126,** 72–77 (1987).
10. F. J. Northrup, G. A. Bethardy, and R. G. Macdonald, *J. Mol. Spectrosc.* **186,** 349–362 (1997).
11. S. Carter, I. M. Mills, and N. C. Handy, *J. Chem. Phys.* **99,** 4379–4390 (1993).
12. A. G. Maki and G. Ch. Mellau, *J. Mol. Spectrosc.* **206,** 47–52 (2001).
13. M. Winnewisser and J. Vogt, *Z. Naturforsch. A* **33,** 1323–1327 (1978).
14. J. Preusser, Ph.D. thesis, Justis-Liebig-University, Giessen, 1994.
15. J. Preusser and A. G. Maki, *J. Mol. Spectrosc.* **162,** 484–497 (1993).
16. A. G. Maki, E. K. Plyler, and R. Thibault, *J. Opt. Soc. Am.* **54,** 869–876 (1964).
17. A. G. Maki, W. Quapp, G. C. Mellau, S. Klee, and S. Albert, *J. Mol. Spectrosc.* **174,** 365–378 (1995).
18. W. Quapp, M. Hirsch, G. C. Mellau, S. Klee, M. Winnewisser, and A. Maki, *J. Mol. Spectrosc.* **195,** 284–298 (1999).
19. A. G. Maki, *Appl. Phys. Lett.* **12,** 122–124 (1968).
20. A. G. Maki and J. S. Wells, "Wavenumber Calibration Tables from Heterodyne Frequency Measurements," NIST Special Publication 821, U.S. Government Printing Office, Washington, DC, 1991. [Also available in updated form via the internet at http://physics.nist.gov/]
21. G. A. Voerkelius, *Chem. Ztg.*, 1078–1081 (1909).
22. B. P. Winnewisser, J. Reinstädtler, K. M. T. Yamada, and J. Behrend, *J. Mol. Spectrosc.* **136,** 12–16 (1989).
23. A. G. Maki, G. C. Mellau, S. Klee, M. Winnewisser, and W. Quapp, *J. Mol. Spectrosc.* **202,** 67–82 (2000).
24. T. Nakagawa and Y. Morino, *Bull. Chem. Soc. Jpn.* **42,** 2212–2219 (1969).
25. T. Nakagawa and Y. Morino, *J. Mol. Spectrosc.* **31,** 208–229 (1969).
26. L. O. Hocker and A. Javan, *Appl. Phys. Lett.* **12,** 124–125 (1968).
27. L. E. S. Mathias, A. Crocker, and M. S. Wills, *IEEE J. Quant. Electron.* **QE-4,** 205–208 (1968).